Journal of Rare Earths 36 (2018) 238–242

Contents lists available at ScienceDirect

Journal of Rare Earths

journal homepage: http://www.journals.elsevier.com/journal-of-rare-earths

Synthesis and optical characterization of Eu^{2+},Tb^{3+}-codoped $Sr_3Y(PO_4)_3$ green phosphors☆

Anxiang Guan, Zuizhi Lu, Fangfang Gao, Xiaoshan Zhang, Huan Wang, Tianjiao Huang, Liya Zhou*

School of Chemistry and Chemical Engineering, Guangxi University, Nanning 530004, China

ARTICLE INFO

Article history:
Received 3 May 2017
Received in revised form
25 June 2017
Accepted 26 June 2017
Available online 25 August 2017

Keywords:
Luminescence
Phosphors
Optical properties
Energy transfer
Rare earths

ABSTRACT

A series of Eu^{2+},Tb^{3+}-codoped $Sr_3Y(PO_4)_3$ (SYP) green phosphors were synthesized by high-temperature solid–state reaction. Several techniques, such as X-ray diffraction, UV–vis spectrum, and photoluminescence spectrum, were used to investigate the obtained phosphors. The present study investigates in detail photoluminescence excitation and emission properties, energy transfer between the two dopants, and effects of doping ions on optical band gap. SYP:0.05Eu^{2+} phosphor shows an intense and broad excitation band ranging from 220 to 400 nm and exhibits a bright green emission band with CIE chromaticity coordinates (0.189, 0.359) under 350 nm excitation. Green emission of SYP:0.03 Tb^{3+} is intensified by codoping with Eu^{2+}, and energy transfer mechanism between them is demonstrated to be a dipole–dipole interaction. Upon 350 nm excitation, SYP:Eu^{2+},Tb^{3+} phosphors exhibits two dominating bands peaking at 466 and 545 nm, which are assigned to $4f^65d^1 \rightarrow 4f^7$ transition of Eu^{2+} ions and $^5D_4 \rightarrow {}^7F_5$ transition of Tb^{3+} ions, respectively. Optimal doping concentrations of Eu^{2+} and Tb^{3+} in the SYP host are 5 mol% and 15 mol%, respectively. Results indicate that SYP:Eu^{2+},Tb^{3+} phosphors are potentially used as green-emitting phosphors for white light-emitting diodes.

1. Introduction

Phosphor-converted white light-emitting diodes (w-LEDs) attracted considerable interest because of their superior lighting and display properties.[1] These diodes fall under two categories: blue (440–470 nm) InGaN and near-ultraviolet (n-UV; 350–420 nm) GaN chips combined with phosphors.[2]

Eu^{2+} ions, as efficient activators in phosphors, are widely investigated owing to their generally strong excitation band, which covers emissions from n-UV LEDs, and intense emission band, which originates from the transition between $^8S_{7/2}$ ($4f^7$) ground state and $4f^65d^1$ excited state configuration. Luminescence wavelength of Eu^{2+} ions can be changed from UV to red depending on crystal field strength and site symmetry.[2,3] Green phosphors are considered factors that affect luminous flux much more significantly than red and blue phosphors.[4] Owing to predominant transition $^5D_4 \rightarrow {}^7F_5$ with green-emitting light at 541 nm, Tb^{3+} is frequently used as activator in numerous hosts. However, excitation spectrum of Tb^{3+} only includes narrow and weak bands in the UV region because of absolute forbiddance of 4f→4f electric dipole transitions, indicating that UV light cannot be absorbed efficiently by Tb^{3+}.[5–7] Utilizing energy transfer from sensitizers to activators is an efficient method to intensify Tb^{3+} absorption in the UV region; numerous researchers used Eu^{2+} as sensitizer for Tb^{3+} in many hosts, such as $Sr_2MgSi_2O_7$:Eu^{2+},Tb^{3+},[8] $Ca_5(PO_4)_3Cl$:Eu^{2+},Tb^{3+}[9] and $Ba_3LaNa(PO_4)_3F$:Eu^{2+},Tb^{3+}.[10]

Phosphate compound is assumed to be ideal for charge stabilization because of its tetrahedral rigid 3D matrix, whereas phosphate phosphors represent a well-known family of luminescent materials with significant potential for w-LEDs.[11,12] Guo et al.[13] reported color-tunable $Sr_3Y(PO_4)_3$ (SYP):Eu^{2+},Mn^{2+} phosphors, but no study reported structure and luminescent properties of Eu^{2+},Tb^{3+}-codoped SYP phosphors to our knowledge. In this study, we synthesized SYP:Eu^{2+},Tb^{3+} using a conventional solid–state reaction. We also investigated photoluminescence (PL) properties and concentration-quenching phenomenon.

☆ **Foundation item**: Project supported by the National Natural Science Foundation of China (61664002) and the Natural Science Foundation of Guangxi Province (2016GXNSFDA380036).

* Corresponding author.
E-mail address: zhouliyatf@163.com (L.Y. Zhou).

http://dx.doi.org/10.1016/j.jre.2017.06.013
1002-0721/

2. Experimental

2.1. Materials and synthesis

In this work, all described $Sr_{2.95}Y_{1-x}(PO_4)_3$:0.05Eu^{2+},xTb^{3+} ($x = 0$, 0.01–0.20) powder samples were synthesized by high-temperature solid–state reaction. For simplicity, $Sr_{2.95}Y_{1-x}(PO_4)_3$:0.05Eu^{2+},xTb^{3+} is hereinafter referred to as SYP:0.05Eu^{2+},xTb^{3+}. High-purity raw materials $SrCO_3$ (A.R.), Y_2O_3 (99.99%), $NH_4H_2PO_4$ (A.R.), Eu_2O_3 (99.99%), and Tb_4O_7 (99.99%) were thoroughly mixed in stoichiometric amounts and then transferred to aluminum crucibles. Mixtures were pre-sintered at 300 °C for 2 h in air and re-sintered at 1300 °C for 4 h under flowing reduction atmosphere of 80% N_2 and 20% H_2. Finally, hard-sintered bodies were crushed into white products for measurement.

2.2. Sample characterization

At 10°–70°, powder X-ray diffraction (XRD) data were collected using a Rigaku D/max-IIIA diffractometer (Cu Kα radiation, $\lambda = 0.15407$ nm). UV–vis absorption spectra of as-synthesized phosphors were examined with a Cary 5000 UV–vis spectrophotometer. During the UV–vis measurement, the as-synthesized phosphor samples were first transferred to the sample chamber, compacted and flattened without using any solvent; then $BaSO_4$ whiteboard was used as integral ball and measuring range is set as 200–700 nm. When star button was pressed, curves starting from 700 to 200 nm gradually emerged and corresponding UV–vis absorption data were collected by data collector connected to computer. PL and PL excitation (PLE) spectra were recorded using a Hitachi F-2500 fluorescence spectrophotometer equipped with a 150 W Xenon lamp as excitation source. All aforementioned measurements were carried out at room temperature.

3. Results and discussion

3.1. Phase formation

Fig. 1 shows XRD patterns of Eu^{2+}/Tb^{3+}-doped and (Eu^{2+},Tb^{3+})-codoped SYP samples. All XRD peaks of the sample series agree well with standard data of SYP (JCPDS card no. 44-0320) except for an impurity peak at 26° (2θ), and the additional weak diffraction peak was identified as the by-product $Sr_3(PO_4)_2$ (JCPDS 24-1008). However, results indicate that dopants posed minimal influence on phase structure of SYP. Radius percentage difference between doped ions (Eu^{2+},Tb^{3+}) and possible substituted ions (Sr^{3+}, Y^{3+}, P^{5+}) were calculated by the following equation[14]; Table 1 summarizes results.

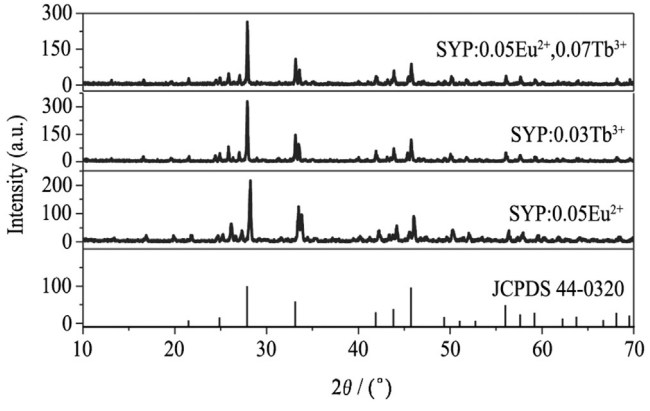

Fig. 1. Powder XRD patterns of SYP doped with different activating agents as compared to the standard data for $Sr_3Y(PO_4)_3$.

$$R_r = 100 \times [R_h(CN) - R_d(CN)]/R_h(CN) \quad (1)$$

where CN refers to coordination number, R_r represents radius percentage difference between doped ions and host ions, and R_h(CN) and R_d(CN) correspond to radius of host cations and doped ions, respectively. According to Ref. 15, Y^{3+} is coordinated with other six atoms. As depicted in Table 1, Eu^{2+} and Tb^{3+} probably substituted Sr^{2+} and Y^{3+} ions in the studied SYP host lattice, respectively. When Sr^{2+} site was replaced by Eu^{2+}, cell volume and d value decreased because the radius of Eu^{2+} is smaller than that of Sr^{2+}. According to Bragg's law,[16] $2d\sin\theta = n\lambda$, and θ is inversely proportional to d; thus, primary diffraction peaks slightly shifted toward a larger 2θ angle with decreasing d value.

3.2. Optical band gap energy

Fig. 2(a) plots UV–vis absorption spectra of pure SYP and Eu^{2+}/Tb^{3+}-activated SYP. All spectra exhibited host absorption edge at approximately 200 nm. As this peak emerged, two other absorption bands extended from 215 to 280 nm and from 280 to 440 nm. Both bands were ascribed to $4f^7$ to $4f^65d^1$ absorption of Eu^{2+} ions in Eu^{2+}/Tb^{3+}-doped SYP. No evident signal of Tb^{3+} was detected as Tb^{3+} ions showed weak absorption in the n-UV/UV region compared with broad and strong absorption of Eu^{2+}. Fig. 2(b) shows the $(\alpha h\nu)^{1/2}$ plot versus photon energy $h\nu$ for rare-earth-ion-doped and undoped samples. The band gap was calculated using the following equation[17]:

$$(\alpha h\nu)^{1/2} \infty (h\nu - E_{gap}) \quad (2)$$

where h refers to Planck's constant, and ν represents light frequency. Energy gap E_{gap} was estimated according to a plot of this equation; the plot was derived from the UV–vis absorption spectra. Optical band gap of pristine SYP host measured 4.6 eV after extrapolating Function (2) to $(\alpha h\nu)^{1/2} = 0$. Similarly, band gaps of other samples were obtained, whereas SYP:0.05Eu^{2+}, SYP:0.05Eu^{2+},0.05Tb^{3+} phosphors exhibited smaller band gap compared with that of pure SYP host. However, band gap energy of SYP:0.03Tb^{3+} was much higher than that of SYP host; this result may be due to increase in cell volume when Y^{3+} was substituted by Tb^{3+}, resulting in decreasing crystal field strength. This result indicates that rare earth ions significantly affected band gap of SYP host.

3.3. PL properties of SYP:Eu^{2+},Tb^{3+} phosphor

Fig. 3(a) shows excitation and emission spectra of the SYP:0.05Eu^{2+} sample. When Eu^{2+} impurity was stoichiometrically added to SYP host, PLE spectra monitored at 416 and 504 nm exhibited similar broad bands in the range of 220–400 nm; these bands were assigned to transitions from ground state $4f^7$ to crystal field split $4f^65d^1$ configuration of Eu^{2+}.[18] The broad extent of excitation spectrum of SYP:0.05Eu^{2+} phosphor matched well with

Table 1
Ionic radii difference between host cations and doped ions.

Ions	CN	Ions radius (nm)	R_r (%)	
			Eu^{2+}(CN = 6, r = 0.117 nm)	Tb^{3+}(CN = 6, r = 0.092 nm)
Sr^{2+}	6	0.118	0.85	21.78
Y^{3+}	6	0.090	−30.00	−2.56
P^{5+}	6	0.038	−207.89	−142.89